Remote Sensing-Based Evapotranspiration Determination: A Review of Single-Source Energy Balance Models

Lehlohonolo Sello[1,] Akhona Maqhubela[1,] and Gaathier Mahed[1]

[1]Department of Geosciences, Nelson Mandela University, Port Elizabeth, 6000, Pormed Lab, Nelson Mandela University, Port Elizabeth, 6000,
gaathier.mahed@gmail.com

DOI: http://dx.doi.org/10.4314/sajg.v11i2.7

Abstract

Remote Sensing evapotranspiration models are critical in order to understand the cycling of water in the environment. Initially, an outline of the concepts related to evapotranspiration, as well as the shortcomings of land-based methods, is presented. The aim of the study was based on reviewing remote sensing evapotranspiration models which provide an alternative data source. These models have proved to be a cheaper alternative to mapping and estimating spatiotemporal evapotranspiration measurements across local and regional scales. This paper reviews the single-source energy balance model, which differs from the two-source model, for estimating spatiotemporal measurements of evapotranspiration. The single-source energy balance model is underpinned by mathematical equations which differentiate the various single-source evapotranspiration models (Surface Energy Balance Systems, Simplified Surface Energy Systems, Surface Energy Balance Algorithm, and Mapping Evapotranspiration at high Resolution and with Internalised Calibration). The soil surface and forest canopy components were observed to be the major difference between the single and dual-source models. Further advice was discussed on the implementation of the OpenET tool, which provides an open and accessible satellite-based estimation of evapotranspiration for improved water management.

Keywords: *Evapotranspiration, Remote sensing, Surface Energy Balance Models*

1. Introduction

Evapotranspiration (ET) is explained as a combination of two processes where water is lost from the surface through evaporation and transpiration, both of which occur when the water gained through uptake by plants is lost via their leaves (Figure 1) (Gibson, 2013; Shoko et al., 2015) (Jovanovic *et al.*, 2015; Ramoelo *et al.*, 2014). South Africa is considered a water-stressed country because the majority of the land is regarded as semi-arid (Gibson, 2013). In arid and semi-arid regions, water in the water budget is predominantly lost through evapotranspiration processes (Jin *et al.*, 2013). Hence, variations in evapotranspiration processes tend to alter the spatial distribution of water sources (Maeda *et al.*, 2011 & Jin *et al.*, 2013). Accurate ET models are therefore necessary to assess the potential impact of these variations. Various single-source energy balance models and their applications were reviewed (Table 1).

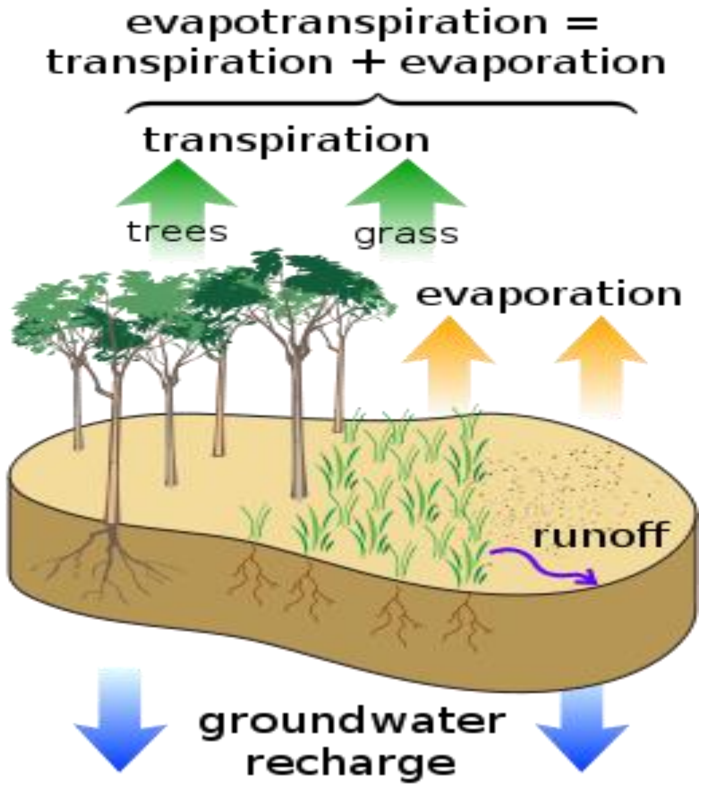

Figure 1: Conceptual diagram of near-surface hydrology, showing evapotranspiration, evaporation, transpiration, runoff, and recharge processes (Adapted after Toews, 2007).

Sharma and Regulwar (2016) argue that conventional methods of estimating ET, which include the water balance, the eddy correlation system, and the Bowen ration are easily accessible on the field scale. However, Liou and Kar (2014) insist that these methods do not allow for accurate estimates of ET on a regional and global scale. In addition, these conventional techniques are expensive to adopt. Remote sensing techniques based on the surface energy balance model (Surface Energy Balance Index, Surface Energy Balance System, Simplified Surface Energy Balance Index, Surface Energy Balance Algorithm, Mapping Evapotranspiration at High Resolution and with Internalised Calibration, Two-Source Models), which provides an alternative to estimating ET on a larger spatial scale and at a lower cost (Gibson *et al*., 2013), were examined.

This paper reviews the single-source energy balance model, which differs somewhat from the two-source models for determining ET (Figure 2). Khand et al. (2019) used a surface energy balance model for estimating spatially distributed ET, especially on varying landscape scales. This uncertainty-limiting approach for reviewing South African ET was proposed in this study in order to enhance the high resolution level encountered during the continuous observation process (Gibson et al., 2011). This study discussed the temporal and spatial variations of regional evapotranspiration measurements to understand ET uniformity on a global scale (Hatfield and Prueger, 2011). This is essential for determining the water balance and the patterns of water utilisation by the vegetation in arid regions (Cristiano *et al.*, 2016). Ground-based evapotranspiration measurements were assessed to understand water balance and water resource management (Park and Choi, 2015). This was essential because the validation of remotely sensed evapotranspiration in the field allows for the utilisation of remotely sensed data with a high degree of certainty (Maes and Steppe, 2012).

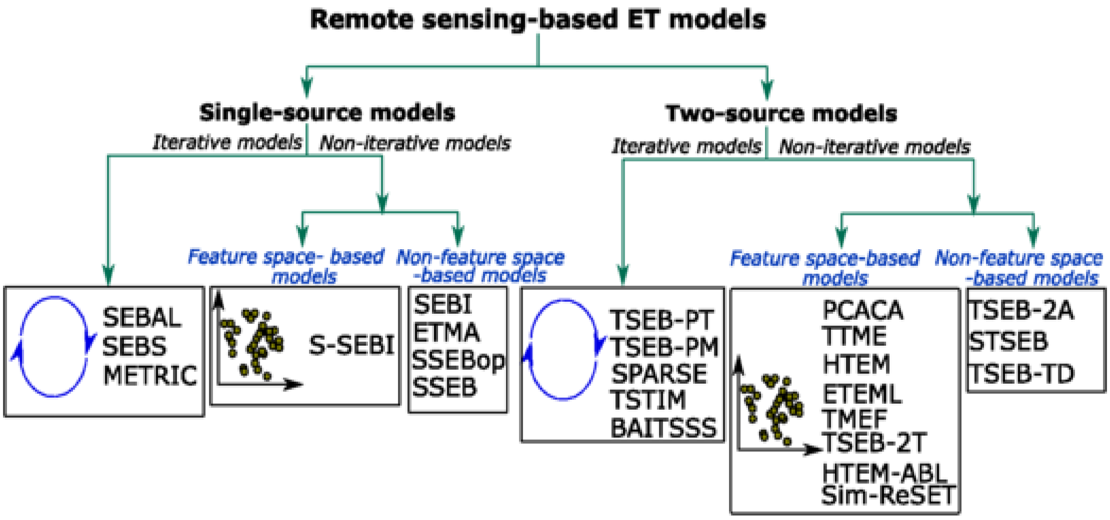

Figure 2: A comparison between single and two-source models for evapotranspiration from remotely sensed data (Prakash Mohan et al., 2020)

2. Energy Balance Model

Surface energy balance models can be divided into two categories: single-source energy balance models and dual-source energy balance models (McShane *et al.*, 2017), Therefore, the analysis of vegetation and soil in a combined energy budget is considered. The surface energy balance equation at the land-air interface, which is based on radiative and turbulent fluxes, is explained in Equation 1 (Roerink *et al.*, 2000). This is broadly applied to both single and dual-source models. The net radiation equation is given as (Hadjimitsis and Papadavid, 2011):

$$R_n = G + H + LE \qquad [1]$$

where G represents the soil heat flux (W.m^{-2}), H the sensible heat flux (W.m^{-2}), and LE the latent heat flux (W.m^{-2}). (L indicates the latent heat of vapourisation and E the actual evapotranspiration)

The sum of the aforementioned parameters equals the net solar radiation. The net solar radiation can be determined from the difference between the incoming solar radiation ($Rs\downarrow$) and the outgoing shortwave solar radiation ($Rs\uparrow$), and the difference between the downwelling atmospheric radiation ($Rs\downarrow$) and the emissivity of the surface, including the reflected long wave radiation ($RL\uparrow$) (Majozi *et al.*, 2017). The radiation balance considers net radiation as the balance between incoming and outgoing radiation under a stable atmosphere (Allen et al., 1998):

$$R_n = R_s \downarrow + R_s \uparrow + R_L \downarrow - R_L \quad [2]$$

where R_n is considered the net radiation ($W.m^{-2}$), $Rs\downarrow$ the incoming short-wave radiation ($W.m^{-2}$), $Rs\uparrow$ the outgoing short-wave radiation ($W.m^{-2}$), and $R_L\downarrow$ the incoming long-wave radiation ($W.m^{-2}$). The net short-wave radiation is given as:

$$\sum R_s = (1-\alpha)R_s \downarrow = (1-\alpha).(S_c \times cos\theta \times d_r \times T_a) \quad [3]$$

where the surface albedo is represented by α, the solar constant by Sc in ($W.m^{-2}$), and the solar incidence angle by θ, the distance between the sun and the Earth by dr, and transmissivity of the atmosphere by T_a.

The incoming long-wave radiation is defined as the thermal radiation flux moving towards the Earth's surface from the atmosphere (Mölg *et al.*, 2009). The emissivity of the air can be quantified as a function of pressure, water vapour, and temperature on cloud-free days:

$$R_L \downarrow = e_{sky} \times \sigma \times T_a^4 \quad [4]$$

where e_{sky} represents the emissivity of the air, σ the Stefan-Boltzamann constant ($W.m^{-2}$), and Ta the air temperature (K). The outgoing long-wave radiation is formulated by applying the Stefan-Boltzmann equation as:

$$R_L \uparrow = \mathcal{E}_0 \times \sigma \times T_s^4 \quad [5]$$

where the surface emissivity is represented by $\mathcal{E}_0$ and the surface temperature (K) by Ts. The sensible heat flux equation can be given as:

$$H = \rho_{air} C_p \frac{dT}{r_{ah}} \quad [6]$$

where ρ_{air} represents the density of the air ($kg.m^{-2}$), C_p the specific air heat, dT the variation between the air temperature and the aerodynamic temperature of the surface, ($dT = T_a - T_s$), and r_{ah} the aerodynamic resistance (Tang *et al.*, 2017). The aerodynamic resistance is defined as a narrow layer of non-turbulent air (about 1mm to 3mm), close to the surface (McMahon *et al.*, 2013). This resistance is termed atmospheric or aerodynamic resistance.

The latent heat flux, which is a component of the net solar radiation equation, is defined as the loss of latent heat from the surface which is due to evapotranspiration (Paul & Aiken, 2013). The latent heat flux is a parameter found in Equation 1 and is given as:

$LE = R_n - G - H$ [7]

3. Review of single-source energy balance models

3.1. Surface Energy Balance Index (SEBI)

In this method, relative evaporation is acquired by raising or diminishing a surface temperature that lies within the maximum range of temperature. This is indicated by high peaks in the surface energy balance, thus denoting theoretical lower and upper bounds in terms of the surface and air temperature variations (Liou and Kumar Kar, 2014). The SEBI algorithm estimates the heat exchange at the land surface by basing it on an estimation of the surface air temperature (Jia *et al.*, 2013). This is helpful as it influences land-surface water and heat exchange during dry and wet periods in semi-arid regions (Gibson *et al*., 2011). Menenti and Choudhury (1993) spearheaded the development related to the parameterization of models of this nature to better determine location-dependent ET

Owing to the restricted availability of water for a specific set of boundary layer characteristics, air temperature in this approach is considered to be zero under dry conditions. This was done to enable the latent heat flux density to assume a maximum value $T_{s,max}$ (maximum surface temperature).

$T_{s,max}$, which is represented in Equation 8, and has been adopted from the bulk transfer equation is given as:

$$T_{s,max} = \langle T \rangle_{pbl} + r_{a,max}\left(\frac{H}{\rho C_p}\right) \quad [8]$$

where the average boundary layer temperature (K) is represented by $<T>_{pbl}$ and the maximum aerodynamic resistance to sensible heat transfer is represented by r_a.

Equation 9 determines the wet region minimum surface temperature by quantifying reference evapotranspiration through the use of the Penman-Monteith equation, which considers no internal resistance:

$$T_{s.min} = \langle T \rangle_{Pbl} + \frac{\frac{r_{a,min}(R_n - G)}{\rho C_\rho} - \frac{e_{sat} - e)}{\gamma}}{1 + \frac{\triangle}{\gamma}} \quad [9]$$

where the minimum aerodynamic resistance in s/m is indicated by $r_{a,min}$, and e and e_{sat} represent actual and saturation vapour pressure, respectively, while the slope of the saturation vapour pressure, as a function of T_a , measured in K Pa/°C, is represented by Δ. The psychometric constant, which is measured in K·Pa/°C, is given as γ. Incorporating the extreme and minimum surface temperatures with the observed surface temperature enables the quantification of the evaporation fraction through the following equation:

$$\frac{LE}{LE_\rho} = 1 - \frac{\triangle T \times r_a^{-1} - \triangle T_{min} \times r_{a,min}^{-1}}{\triangle T_{max} \times r_{a,max}^{-1} - \triangle T_{min} \times r_{a,min}^{-1}} \quad [10]$$

where $\Delta T = Ts - Tpbl$, $\Delta Tmin = Ts, - Tpbl$, and $\Delta Tmax = Ts,max - Tpbl$.

3.2. Surface Energy Balance System (SEBS)

This model was developed by Su (2002) to determine, with the use of ancillary meteorological data, the surface evaporation fraction and turbulent fluxes from satellite imaging systems computing data in the visible, near-infrared, and thermal-infrared range.

In this model, the dry limit value is considered to be zero for the latent heat flux, which implies that the sensible heat flux reaches its maximum value, for example, $H_{dry} = R_n - G$. On the contrary, when evapotranspiration takes place at the wet limit, the evapotranspiration occurs at a potential rate (LE_{wet}), whilst the sensible heat flux retains its minimum value of H_{wet}. The sensible heat flux at the dry and wet limits is represented in Equations 11 and 12 as:

$$H_{dry} = R_n - G \quad [11]$$

$$H_{wet} = R_n - G - LE_{wet} \quad [12]$$

where the r_a relies heavily on the Obukhov length, which is a function of the sensible heat flux and the friction velocity. The Obukhov length is expressed in Equation 13 (Parlange. and Katul, 1995; Su, 2002; Gibson, 2013):

$$L = -\frac{\rho C_{pu_*^3 \theta_v}}{KgH} \quad [13]$$

Where ρ is the density of the air, Cp is the specific heat at a constant temperature, $u*$ is the frictional velocity, K is the von Karman's constant, which is the value of 0.4, g is acceleration due to gravity, H is the specific sensible heat flux, and θ_v is defined as the potential virtual temperature close to the surface. The evaporative fraction (EF) and relative evaporative fraction (EF_r) can be given as:

$$EF = \frac{EF_r \times LE_{wet}}{R_n - G} \quad [14]$$

$$EF = \frac{EF_r \times LE_{wet}}{R_n - G} \quad [15]$$

This method uses satellite earth observation data to estimate turbulent heat fluxes and evaporative fraction with acceptable accuracy (Su, 2002). McCabe et al. (2017) noted that the SEBS model is more sensitive to the quality of the input data than SEB models with less data (Senkondo *et al.*, 2019). SEBS has been extensively applied with MODIS data products and thermal bands over spatially large heterogenous areas distributed across Southern Africa (Gibson, 2013; Shoko *et al.*, 2015). Su (2002) suggests that SEBS involves a credible and independent approach, which enables its results to be used to validate and initialise hydrological, atmospheric, and ecological models.

3.3. Simplified Surface Energy Balance Index (S-SEBI)

The Simplified Surface Energy Balance Index (S-SEBI) is a sequel of SEBI. S-SEBI needs spectral radiances scanned under clear skies in the spectral range of the visible, near-infrared, and thermal band (Roerink *et al.*, 2000). This will aid in acquiring remotely sensed parameters of surface temperatures, vegetation indices, and surface albedo's (Gibson *et al.*, 2011).

The S-SEBI makes use of an evaporative fraction, which is derived from the wet and dry regions of the raster image and developed by combining the reflection-dependent surface temperature between the reflection-dependent minimum and maximum surface temperature (Li *et al.*, 2009; Roerink *et al.*, 2000), as indicated in Equation 16.

$$EF = \frac{(T_H - T_s)}{(T_H - T_{LE})} \quad [16]$$

where the surface temperature T_H corresponds with dry pixels and indicates the minimum latent heat flux ($LE_{dry} = 0$) and the maximum latent heat flux is $H_{dry} = R_n - G$. The surface temperature, which corresponds with the wet pixels is represented by T_{LE}, and also represents the minimum sensible heat flux ($H_{wet} = 0$) and the maximum latent heat flux ($LE_{wet} = (Rn - G)$) for a given surface albedo. Through the use of the regression equation, T_{LE} and T_H can be calculated as:

$$T_{LE} = C_{min} + d_{min}\alpha \quad [17]$$

$$T_H = C_{max} + d_{max}\alpha \quad [18]$$

where the scatter plot of T_s and α is used to calculate the empirical coefficients of $Cmax$, $dmax$, $Cmin$ and dmi over the entire study area.

3.4. Surface Energy Balance Algorithm for Land (SEBAL)

SEBAL, developed by Bastiaanssen et al. (1998) in the Netherlands, relies on a satellite imaging system which computes data in the near visible (0.4 to 0.7 μm), near-infrared (0.7 to 3.0 μm) and thermal-infrared band (3 to 14 μm).Kalma *et al.*, 2008). Together with ground-based ancillary weather data in terms of humidity, wind speed, air temperature and solar radiation *(Ahmad et al.*, 2006) SEBAL can accurately estimate spatial variations in the measurement of evapotranspiration (Bastiaanssen *et al.*, 1998).

This model enables the quantification of values associated with the surface temperature (dT) for each pixel. SEBAL acknowledges the occurrence of a linear relationship between the radiometric surface temperature (T_s) and the near-surface temperature (dT) by considering the surface and homogenous meteorological conditions:

$$dT = cTs + d \quad [19]$$

where c and d are considered to be the empirical coefficients acquired from an anchor point (wet and dry) for a specific satellite image (Bastiaanssen, 1995).

3.5. Mapping evapotranspiration at high resolution and with an internalised calibration (METRIC)

METRIC is a version of SEBAL, which is an energy balance model developed by Allen et al. (2005). It is based on the well-known SEBAL Model (Bastiaanssen *et al.*,1998) in the Netherlands to estimate land surface evapotranspiration from the satellite-based energy balance (Olmedo and Fuente-Saiz, 2018). This model can be considered as an image-processing approach as it implements a residual method to calculate actual evapotranspiration maps (Spiliotopoulos *et al.*, 2017).

Land surface temperature is a key variable in the surface-atmosphere exchange of energy and water (Johannsen *et al.*, 2019). This approach employs an innovative calibration to overcome biases in the retrieval of land surface temperatures during the estimation of the sensible heat flux (Hendrickx and Hong, 2005). The internal calibration of this model minimises errors associated with determining surface roughness and correcting aerodynamic stability (Allen *et al*., 2005).

4. Conclusions

Model	**Specialty regarding H estimation**	**Strength**	**Weakness**	**Suitable scale of operation**	**Time resolution**	**Sensors used**	**Validation**
SEBI63	EF to estimate H H	Suitable when wet and dry pixels are not available in the study area	Meteorological variables from the upper boundary of PBL required	Regional	D	ETM+ and ASTER	Ground-based EF63
S-SEBI57	EF to estimate H H	Image-based	Need constant atmospheric conditions	Basin	D and M	ETM+, MODIS, ASTER, AVHRR, TM5, and OLI-TIRS	EC,57 LAS,57 and BR109
SEBAL 19	Use of near-surface temperature gradient	Calibration by CIMEC	Subjective judgment of calibration pixels	Field to regional	D, M, S, and Y	ETM+, MODIS, ASTER, AVHRR, TM5, and OLI-TIRS	EC,54 LAS,110 LM,111 and BR112
METRIC21	Use of near-surface temperature gradient	Soil moisture at hot pixel considered	Subjective judgment of calibration pixels	Field to regional	D, M, S, and Y	ETM+, TM5, OLI-TIRS, and MODIS	EC,55 LAS,110 LM,111 and BR109

Table 1. Various single-source energy balance models and their applications

The use of the various single-source models, as well as aspects of their application, has been outlined. It should be noted that the major difference between single and dual-source models is the fact that the soil surface and forest canopy components are partitioned (Prakash-Mohan et al., 2020). Table 1 summarizes various single-source energy balance models and their applications. This summary has in fact achieved the objective of this study, namely a review of remote sensing evapotranspiration models.

On the other hand, multi-source models are able to differentiate in greater detail between various components of ET (Athira et al., 2020). The application of single-source models in a South African context is of great importance, largely on account of the semi-arid nature of the majority of the country and, thus, of minimal land cover.

5. The Future of Evapotranspiration modelling

The development of remote sensing techniques has enabled studies to consider implementing various ET estimation algorithms over large areas. The ability to scale this down with tools such as Cube Satellites and Unmanned Aerial Vehicles is becoming easier (Aragon et al., 2018). This type of technology, coupled with open source tools and data, will help in the better management of water resources, particularly for agricultural purposes, by increasing the spatial and temporal resolution (Figure 3).

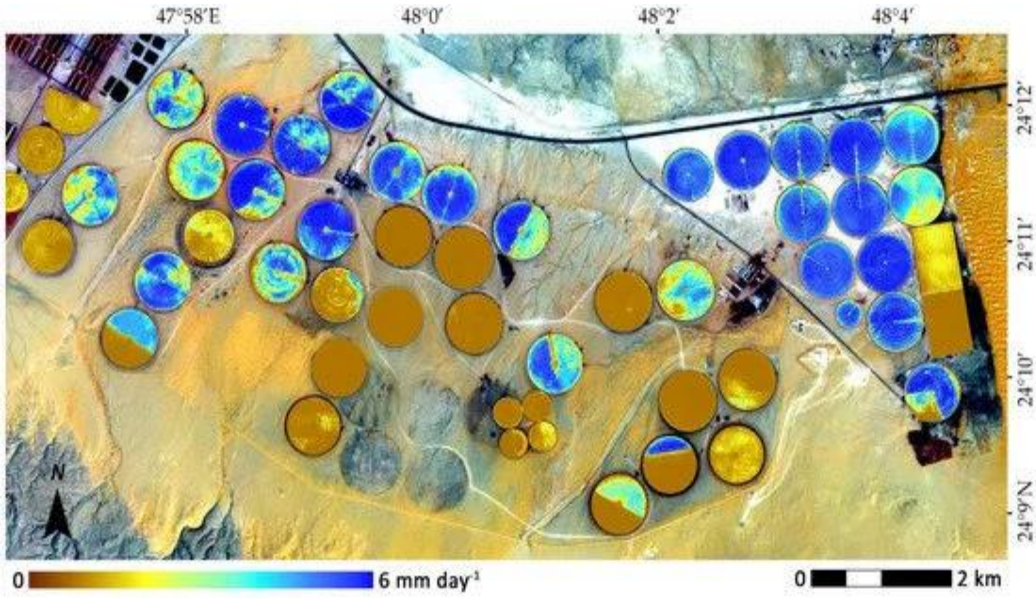

Figure 3: High precision spatial mapping of evapotranspiration from crop circles in an arid environment (Aragon et al., 2018)

One such tool is the OpenET database. The implementation of the OpenET tool provides room for open and accessible satellite-based estimations of evapotranspiration for improved water management. The water supply for agriculture, populations, and ecosystems is efficiently sustainable through the OpenET initiative, as this platform is able to develop an accurate water budget. The consideration of this platform improves and solves many water issues, including those experienced during drought seasons since it supports the financial viability programmes of farms. The tool is, however, only available at this stage in North America hence this study is proposing this programme as a tool to be considered on a global scale.

6. Acknowledgements

We would like to thank the NRF and DST for funding the authors and their bursaries for studies.

7. References

Ahmad, M., Biggs, T., Turral, H., Scott, C.A., 2006, Application of SEBAL approach and MODIS time-series to map vegetation water use patterns in the data-scarce Krishna river basin of India, 83–90.

Allen, R.G., Tasumi, M., Morse, a, Trezza, R., 2005, 'A Landsat-based energy balance and evapotranspiration model in Western US water rights regulation and planning.' Irrigation and Drainage Systems no. 19, 251–268.

Allen, Richard G, Pereira, L.S., Raes, D., Smith, M., Ab, W., 1998, 'Crop evapotranspiration - Guidelines for computing crop water requirements' - FAO Irrigation and Drainage Paper 56, 1–15.

Aragon, B., Houborg, R., Tu, Fisher, McCabe, M. 2018. Cubesats enable high spatiotemporal retrievals of crop water use for precision agriculture, Remote Sensing, 10 (12), 1867

Athira (2020), IEEE

Bastiaanssen, W.G.M., 1995, Regionalization of surface flux densities and moisture indicators in composite terrain: a remote sensing approach under clear skies in Mediterranean climates. Doctoral thesis, Wageningen Agricultural University, Wageningen, The Netherlands.

Bastiaanssen, W.G.M., Menenti, M., Feddes, R.A., Holtslag, A.A.M., 1998a. A remote sensing surface energy balance algorithm for land (SEBAL) 213, 198–212.

Bastiaanssen, W.G.M., Noordman, E.J.M., Pelgrum, H., Davids, G., Thoreson, B.P., Allen, R.G., 2005, SEBAL Model with Remotely Sensed Data to Improve Water Resources Management under Actual Field Conditions, 85–93.

Cristiano P.M., Pereyra D.A., Bucci S.J., Madanes N., Scholz F.G., and Goldstein G., 2016 'Remote Sensing and ground-based measurements of evapotranspiration in an extreme cold Patagonian Desert.' June 2016, Hydrological Process/ Volume 30, Issue 24.

Gibson L., Munch Z., Carstens M., and Conrad J., 2011, 'Remote Sensing Evapotranspiration (SEBS) Evaluation using Water Balance'. June 2011, Water Research Commission. WRC Report No. KV 272/11.

Gibson, L., Jarmain, C., Su, Z., Eckardt, F.E., 2013, Estimating evapotranspiration using remote sensing and the Surface Energy Balance System - a South African perspective: review. Water SA 39, 477–484.

Gibson, L.A., 2013, The Application of the surface energy balance system model to estimate evapotranspiration in South Africa.

Gibson, L.A., Jarmain, C., Su, Z., Eckardt, F.E., 2013, Estimating evapotranspiration using remote sensing and the Surface Energy Balance System – A South African perspective, 39, 477–484.

Hatfield, J., and Prueger, J.H., 2011, Spatial and Temporal Variation in Evapotranspiration. November 2011.

Hendrickx, J.M.H., and Hong, S.H., 2005, Mapping Sensible and latent heat fluxes in arid areas using optical imagery. May 2005, Proceedings of SPIE – The International Society for Optical Engineering 5811.

Jia, D.U., Kaishan, S., Zongming, W., Bai, Z., Dianwei, L.I.U., 2013, Evapotranspiration Estimation Based on MODIS Products and Surface Energy Balance Algorithms for Land (SEBAL) Model in Sanjiang Plain, Northeast China 23, 73–91.

Jin, X., Guo, R., Xia, W., 2013, Distribution of actual evapotranspiration over Qaidam basin, an Arid area in China. Remote Sensing. 5, 6976–6996.

Johannsen, F., Ermida, S., Martin, JPA., Trigo, IF., Nogueira, M., and Dutra, E., 2019, Cold Bias of ERA5 Summertime Daily Maximum Land Surface Temperature over Iberian Peninsula. Remote Sensing. 2019, 11 (21), 2570.

Jovanovic, N., Mu, Q., Bugan, R.D.H., Zhao, M., 2015, Dynamics of MODIS evapotranspiration in South Africa, Water SA, 41, 79–90.

Kalma, J.., McVicar, T.., Mccabe, M.F., 2008, Estimating Land Surface Evaporation: A Review of Methods using Remotely Sensed Surface Temperature Data. Survey Geophysics 421–469.

Khand, K.., Taghvaeian, S.., Gowda, P., and Paul, G., 2019, A modeling framework for deriving daily time series off evapotranspiration maps using a surface energy balance model. Remote Sensing 11 (5), 508, 2019.

Liou Y., and Kar S.K., 2014, Evapotranspiration Estimation with Remote Sensing and Various Surface Energy Balance Algorithms – A Review. Center for Space and Remote Sensing Research, Energies 2014, 7, 2821-2849.

Maeda, E.E., Wiberg, D.A., Pellikka, P.K.E., 2011, Estimating reference evapotranspiration using remote sensing and empirical models in a region with limited ground data availability in Kenya. Applied Geography. 31, 251–258.

Maes W.H., and Steppe K., 2012, 'Estimating evapotranspiration and drought stress with ground-based thermal remote sensing in agriculture: a review.' *Journal of Experimental Botany*, Volume 63, Issue 13, August 2012, 4671-4712.

Majozi, N.P., Mannaerts, C.M., Ramoelo, A., Mathieu, R., Mudau, A.E., Verhoef, W., 201, An intercomparison of satellite-based daily evapotranspiration estimates under different eco-climatic regions in South Africa. Remote Sensing. 9, 1–21.

McCabe, M.R., Alsdorf, D.E., Miralles, D.G., Uijlenhoet, R., Wagner, W., Lucieer, A., Houborg, R., Niko E. C. Verhoest, Trenton E. Franz, J.S., Gao, H., Wood, E.F., 2017, 'The Future of Earth Observation in Hydrology. 'Hydrology and Earth System Sciences. Hydrological Earth Systems Sciences. Under review, 3879–3914.

McShane R.R., Driscoll K.P., and Sando R., 2017, 'A Review of Surface Energy Balance Models for Estimating Actual Evapotranspiration with Remote Sensing at High Spatiotemporal Resolution over Large Extents.' Scientific Investigations Report, 2017-5087.

Mölg, T., Cullen, N.J., Kaser, G., 2009, Solar radiation, cloudiness and longwave radiation over low-latitude glaciers: Implications for mass-balance modelling. Journal of Glaciology. 55, 292–302.

Mementi M. and Choudhury, B. 1993, Parameterization of land surface evaporation by means of location dependent potential evaporation and surface temperature range.

Park, J., and Choi, M., 2015, Estimation of Evapotranspiration from ground-based meteorological data and global land data assimilation system (GLDAS). Stochastic Environmental Resources Risk Assessment 29, 1963-1992

Parlange, Marc B. and Katul, G.G., 1995, Watershed scale shear stress from tethersonde wind profile measurements under near neutral and unstable atmospheric stability.

Paul, G., Aiken, R.M., 2013, Role of hot and cold pixel concept in remote sensing-based single-source energy balance algorithms using 21st Century Technology to better manage irrigation water supplies. Seventh International Conference on Irrigation and Drainage

Prakash-Mohan, M.M., 2020, Review of approaches for the estimation of sensible heat flux in remote sensing-based evapotranspiration models, Journal of Applied Remote Sensing, 14 (4), 041501.

Ramoelo, A., Majozi, N., Mathieu, R., Jovanovic, N., Nickless, A., Dzikiti, S., 2014, Validation of Global Evapotranspiration Product (MOD16) using Flux Tower Data in the African Savanna, South Africa 7406–7423.

Roerink, G.J., Su, Z., Menenti, M., 2000, 'S-SEBI: A simple remote sensing algorithm to estimate the surface energy balance.' Physics and Chemistry of the Earth, Part B Hydrology Ocean Atmosphere. 25, 147–157.

Senkondo W., Munishi S.E., Tumbo M., Nobert J., and Lyon S.W., 2019, Comparing Remotely-sensed Surface Energy Balance Evapotranspiration Estimates in Heterogeneous and Data-limited Regions: a Case Study of Tanzania's Kilombero Valley. May 2019, 11, 1289.

Sharma, S., and Regulwar, D. 2016, 'Prediction of Evapotranspiration by Artificial Neural Network and Conventional Methods.' *International Journal of Engineering Research*, 5 (1).

Shoko, C., Dube, T., Sibanda, M., Adelabu, S., 2015, Applying the Surface Energy Balance System (SEBS) remote sensing model to estimate spatial variations in evapotranspiration in Southern Zimbabwe. Transactions of the Royal. Society of South Africa 70, 47–55.

Spiliotopoulos, M., Holden, N.M., and Loukas, A. 2017, 'Mapping Evapotranspiration Coefficients in a Temperate Maritime Climate using the METRIC Model and Landsat TM.' Volos, 382 21, Greece. Water. 2017, 9 (1), 23.

Su, Z., 2002, 'The Surface Energy Balance System (SEBS) for estimation of turbulent heat fluxes'. Hydrology and Earth System Science. 6, 85–100.

Tang R., and Li Z. L., 2017, Estimating Daily Evapotranspiration from Remotely Sensed Instantaneous Observations with Simplified Derivations of a Theoretical Model. September 2017, *Journal of Geophysics Research*: Atmosphere. Volume 122, Issue 19.

Toews M.W., 2007, Conceptual diagram of near-surface hydrology, showing evapotranspiration, evaporation, transpiration, runoff, and recharge processes.

Olmedo, GF., and Fuente-Saiz, DDL., 2018, Surface Energy Balance using METRIC Model and Water package: 1. Simple procedure.